JACS
JOURNAL OF THE AMERICAN CHEMICAL SOCIETY

COMMUNICATION

pubs.acs.org/JACS

Sticky Interconnect for Solution-Processed Tandem Solar Cells

Vincent C. Tung, Jaemyung Kim, Laura J. Cote, and Jiaxing Huang*

Department of Materials Science and Engineering, Northwestern University, Evanston, Illinois 60208, United States

Supporting Information

ABSTRACT: Graphene oxide (GO) can be viewed as a two-dimensional, random diblock copolymer with distributed nano-size graphitic patches and highly oxidized domains, thus capable of guiding the assembly of other materials through both $\pi-\pi$ stacking and hydrogen bonding. Upon mixing GO and conducting polymer poly(3,4-ethylenedioxythiophene):poly(styrenesulfonate) (PEDOT:PSS) in water, a dispersion with dramatically increased viscosity is obtained, which turns into sticky thin films upon casting. Surprisingly, the insulating GO makes PEDOT much more conductive by altering its chain conformation and morphology. The GO/PEDOT gel can function as a metal-free solder for creating mechanical and electrical connections in organic optoelectronic devices. As a proof-of-concept, polymer tandem solar cells have been fabricated by a direct adhesive lamination process enabled by the sticky GO/PEDOT film. The sticky interconnect can greatly simplify the fabrication of organic tandem architectures, which has been quite challenging via solution processing. Thus, it could facilitate the construction of high-efficiency tandem solar cells with different combinations of solution-processable materials.

Graphite oxide sheets, now called graphene oxide (GO), result from chemical exfoliation of graphite by a process that has been known for more than a century.[1,2] With oxygenated functional groups attached to its basal plane and edges, GO can be readily dispersed in water. Interest in this old material resurged in 2004,[3] and GO has been extensively pursued as a solution-processable precursor for bulk production of graphene.[4−8] Apart from making graphene, GO itself has many intriguing properties. Like graphene, GO sheets are characterized by two abruptly different length scales. The measured thickness is of typical molecular dimensions (~1 nm),[9] but the lateral dimensions are those of common colloidal particles, ranging from nanometers[10] up to hundreds of micrometers.[11] Therefore, GO sheets can be viewed as either molecules or particles, depending on which length scale is of greater interest. On the other hand, GO can be characterized as an unconventional soft material[12−15] such as a two-dimensional (2D) polymer, anisotropic colloid, membrane, liquid crystal,[16] or amphiphile.[12−15] Earlier structural models[17,18] and recent high-resolution transmission electron microscopy studies[19] suggest that the basal plane of a GO sheet is composed of unoxidized graphitic patches and heavily oxidized domains functionalized by hydroxyl and epoxide groups (Figure S1a (Supporting Information)). Therefore, when interacting with other materials, GO can act as a 2D random diblock copolymer with the two blocks capable of $\pi-\pi$ stacking and hydrogen bonding, respectively. To explore how such 2D diblock scaffold guides assembly, here we report the synergistic coassembly of GO and poly(3,4-ethylenedioxythiophene):poly(styrenesulfonate) (PEDOT:PSS) (Figure S1b), which is a widely used conducting polymer in organic optoelectronic devices.[20] Although GO is well dispersed in water and electrically insulating, adding GO to PEDOT:PSS can dramatically increase the solution viscosity and the electrical conductivity of the resulting composite, thus forming a conductive glue. Upon casting, the gel turns into an adhesive, transparent, and conducting thin film which is well suited for mechanically and electrically connecting parts in organic electronic devices. As a proof-of-concept, here we demonstrate its use as the sticky interconnect to create solution-processed tandem solar cells through a direct adhesive lamination (i.e., gluing) process.

Tandem solar cells are multijunction photovoltaic devices in which two subcells are stacked to achieve higher overall solar absorption. If connected in series, this leads to a higher open-circuit voltage (V_{oc}) equal to the sum of those of the subcells, thus increasing the overall power conversion efficiency. In parallel to the rapid progress in the material design and engineering of the light-absorbing layer, tandem device architectures have attracted great interest for organic solar cells.[21−26] For inorganic photovoltaic systems, tandem architecture can be more conveniently fabricated by sequential evaporation steps, which has already achieved great success. However, its progress in organic solar cells, especially in solution-processed ones, has been limited, primarily due to the complexity encountered during multiple solution deposition steps.[21,22] The interconnect layer that separates the two subcells, for example, needs to be made with sufficient conductivity, high transparency, low surface roughness, dense coverage, and high mechanical and chemical stability. More importantly, the interlayer material needs to have orthogonal processability to maintain the stacking integrity and avoid intermixing between the different layers in the device. It should be processed in a solvent that will not affect the underlying subcell, and at the same time it should withstand the solvent used to deposit the top subcell. These material-processing challenges are a major roadblock in the widespread study of tandem structure in solution-processed solar cells.[21,22] The water-processable GO/PEDOT gel associated with the direct adhesive lamination process we report here can potentially eliminate the constraint imposed by orthogonal processability, thus greatly simplifying the device fabrication of tandem structures.

GO was prepared by a modification of Hummers' method[2] and extensively washed to remove the salt byproduct and excess acid.[27] The dried GO filter cakes were then redispersed in water

Received: April 14, 2011
Published: May 26, 2011

dx.doi.org/10.1021/ja203464n | J. Am. Chem. Soc. 2011, 133, 9262–9265

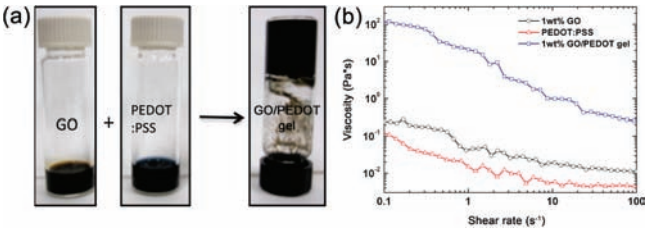

Figure 1. (a) Gelation occurs upon mixing aqueous dispersions of GO and PEDOT:PSS, as shown in the "no flow" test. The final GO concentration is 1 wt %. (b) Viscosity measurements at 20 °C show over 2 orders of magnitude increase in viscosity upon mixing.

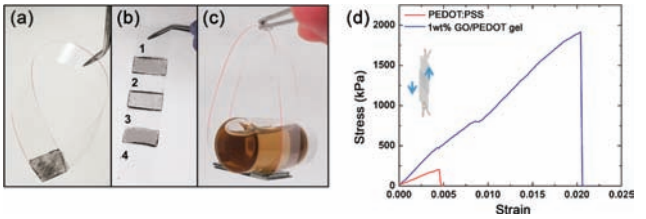

Figure 2. Dried GO/PEDOT:PSS gel makes a sticky adhesive for (a) PET ribbon and (b) glass slides. (c) A vial of 20 mL of GO in water can be supported by a platform glued together by the gel. (d) Shear stress−strain curves of two PET stripes glued together by GO/PEDOT gel (blue) and PEDOT:PSS (red), respectively. The inset shows the geometry of measurement.

to prepare colloidal dispersions with various concentrations up to 2 wt %. PEDOT:PSS aqueous dispersion (1.3−1.7 wt %) was used as received. Significantly increased solution viscosity was noted upon adding GO dispersions (0.1−2 wt %) into PEDOT:PSS. With 1 wt % GO added, the solution turned into a solid gel that can sustain the vial inversion test (Figure 1a). Figure 1b shows the viscosity measurements of GO, PEDOT:PSS, and their mixture. Indeed, the gel has 2−3 orders of magnitude higher viscosity at all shear rates. Additional measurements (Figure S1c) showed that 1−2 orders of magnitude increase in viscosity can be achieved with only 0.1 wt % GO in the blend. For GO dispersions, only a moderate increase in viscosity was recorded when the concentration increased from 0.1 to 1 wt %. Therefore, gelation suggests strong interactions between GO and PEDOT:PSS. In control experiments (Figure S1c), mixing GO and PSS (1 wt %) did not result in gelation nor apparent increase in viscosity since they both are negatively charged and would not be able to cross-link. Therefore, it should be the interaction between GO and PEDOT that is responsible for the gelation. Thus, hereinafter the mixture of GO and PEDOT:PSS is referred to as GO/PEDOT gel for brevity. The viscosity of GO/PEDOT gel can be reversibly tuned by temperature (Figure S2), suggesting noncovalent interactions between GO and PEDOT, most likely $\pi-\pi$ stacking and hydrogen bonding.

The GO/PEDOT gel can be readily applied onto a variety of substrates including silicon wafer, glass, and common plastics to form thin films. Drying the films under mild heating at 60 °C can turn them into sticky adhesives. Figure 2a shows a strip of poly(ethylene terephthalate) (PET) film glued together at the ends to form a knot. In Figure 2b, a 10 cm long glass bridge was made by gluing four glass slides together. In Figure 2c, the two ends of a PET strip were sandwiched and glued between two glass slides to form a platform capable of supporting a vial containing

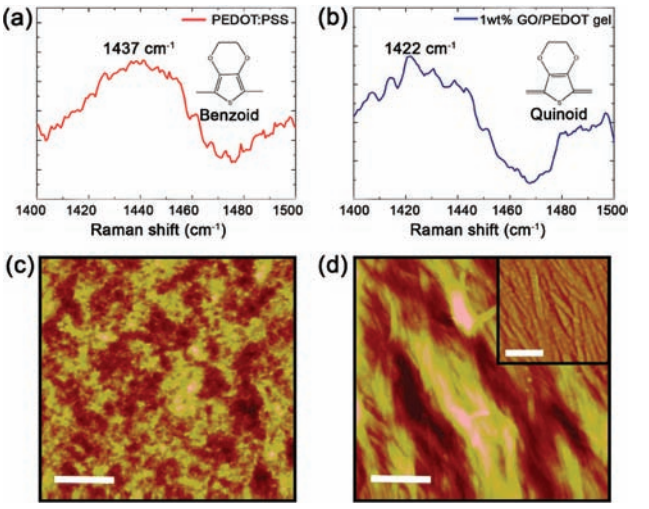

Figure 3. (a,b) Raman spectra suggest a benzoid−quinoid transition in the thiophene unit of PEDOT upon interacting with GO. (c,d) AFM images reveal that adding GO changes the morphology of PEDOT:PSS thin film from (c) particulate to (d) fibril. The inset in (d) shows aligned fibrillar domains with diameters of ∼100 nm. Scale bar = 5 μm. Inset scale bar = 500 nm. The changes in chain confirmation and morphology are responsible for dramatically increased electrical conductivity.

20 mL of GO solution. Stress−strain responses of PET stripes glued together with GO/PEDOT gel and PEDOT:PSS were measured in shear direction (Figure 2d). The stripes with PEDOT:PSS glue can withstand a maximum stress of 0.2 MPa, with a maximum displacement of about 0.5%. Adding 1 wt % GO to the PEDOT:PSS resulted in approximately 10 times maximum stress and 4 times maximum displacement. It was also found that GO dispersion itself cannot glue PET stripes together. The moderate increase in the slope of the stress−strain curves in Figure 2d suggests that PEDOT:PSS was slightly stiffened upon mixing with GO.

In addition to highly increased viscosities, adding GO to PEDOT:PSS also results in dramatically enhanced electrical conductivity of the composite. Four point−probe measurements showed that the unannealed PEDOT:PSS thin films have very low conductivity, ∼0.025 S/cm. However, GO/PEDOT films showed over 1 order of magnitude improvement, with conductivity ∼0.4 S/cm. In a different geometry, depositing a layer of GO on top of PEDOT:PSS can also increase the polymer's conductivity by nearly 1 order of magnitude (Figure S3). Although a number of reports have shown enhanced conductivity of PEDOT:PSS by adding a *conductive* form of graphene-based sheets,[28−31] the conductivity enhancement by an *insulating* GO is unexpected and should have a fundamentally different mechanism. We hypothesize that it is due to a conformational change of PEDOT upon its interaction with GO. PEDOT has two resonating ground-state conformations, namely benzoid and quinoid states. The benzoid−quinoid transition can increase the conductivity of PEDOT:PSS.[32] The two ground states can be identified by a Raman signature of the $C_\alpha-C_\beta$ stretching mode in the thiophene ring between 1400 and 1500 cm^{-1}. Figure 3a,b shows that the $C_\alpha-C_\beta$ stretching band indeed red-shifted from 1437 to 1422 cm^{-1} upon addition of GO, suggesting that the PEDOT polymer is becoming more quinoidal, and thus more conductive. This could also explain the increased stiffness of the PEDOT polymer as shown in Figure 2d, since quinoidal PEDOT

dx.doi.org/10.1021/ja203464n |*J. Am. Chem. Soc.* 2011, 133, 9262–9265

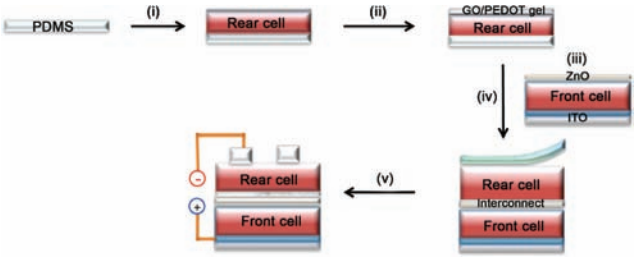

Figure 4. Schematic diagram illustrating the construction of a polymer tandem solar cell using the GO/PEDOT sticky interconnect. (i) The active layer of the rear cell is first spin-cast onto a PDMS stamp. (ii) GO/PEDOT gel is spin-coated on top of the active layer. (iii) A ZnO layer is spin-coated on top of a separately prepared front cell as part of the interconnecting layer. (iv) The rear cell is directly glued to the front cell. Subsequential annealing at 150 °C can convert GO to the more conductive reduced GO and improve the adhesion between the two subcells. (v) Finally, the PDMS stamp is peeled off for thermal evaporation of the top metal electrodes.

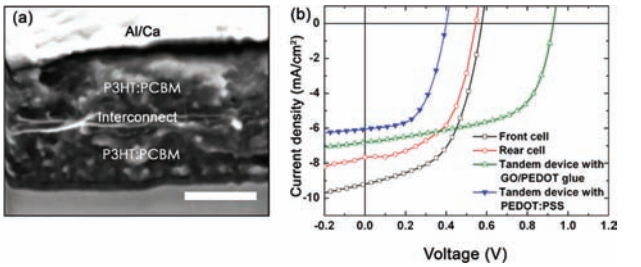

Figure 5. (a) Cross-sectional SEM image of an as-fabricated tandem device. The two subcells and the interconnect layer can be clearly distinguished. Scale bar = 150 nm. (b) $I-V$ characteristics of separately prepared front cell (black) and rear cell (red) along with tandem cells laminated with PEDOT:PSS only (blue) and GO/PEDOT gel (green), respectively.

is indeed more rigid. Atomic force microscopy (AFM) images revealed that the PEDOT thin films changed from granular (Figure 3c) to fibrillar (Figure 3d) after addition of GO, likely due to more-rigid chains. The inset of Figure 3d shows that the nanofibrillar domains are well aligned, which can also help to increase the conductivity of the polymer.

Since PEDOT:PSS is one of the most widely used conducting polymers in organic electronics,[20] making it more conductive and sticky should enable its use as nonmetallic solder for interconnecting different elements in devices. The GO/PEDOT thin films can be made highly transparent (Figure S4a), conductive, and adhesive. Moreover, gentle thermal annealing (150 °C) can make the GO/PEDOT thin film even more conductive through the combined results of cross-linking PEDOT:PSS[20] and reducing GO.[33] This makes the glue well suited for connecting elements in multilayer optoelectronic devices. Here, we demonstrate that GO/PEDOT gel can be used as a sticky interconnect layer for constructing solution-processed tandem polymer solar cells through a direct lamination process. Fabrication of solution-processed polymer tandem cells has been challenging. A major problem is the stacking integrity of different subcells during multiple solution-casting steps. If good contact can be achieved between the interconnect layer and the two neighboring subcells, a direct lamination process would be highly desirable, as it eliminates most of the solution-processing problems. To achieve the highest efficiency, typically two polymers with complementary light absorption are used in a tandem cell. However, to facilitate the evaluation of the sticky GO/PEDOT interconnect, the same polymer can be used for both subcells in order to minimize any interference that may potentially be induced by fabricating cells with different polymers. We chose the prototypical poly(3-hexylthiophene) (P3HT) and phenyl-C_{61}-butyric acid methyl ester (PCBM) bulk heterojunction devices as our standard cell since they have been developed to a relatively mature stage.[21] The value of V_{oc} is the key parameter to evaluate the successful connection of the two subcells. With two identical subcells, the resulting tandem device should have a doubled V_{oc}. If intermixing between the two subcells occurs, the V_{oc} would decrease and could be even lower than that of the subcell.

Figure 4 shows the architecture of the device after each step of fabrication. First, the P3HT:PCBM active layer (130 nm) of the rear cell is spin-cast from its chloroform solution onto a polydimethylsiloxane (PDMS) stamp. A GO/PEDOT layer (10 nm) is then spin-coated on top of this active layer using its aqueous dispersion. In parallel, a front cell was fabricated by spin-coating P3HT:PCBM (150 nm) from its dichlorobenzene solution on a PEDOT:PSS modified indium tin oxide substrate. The front cell is further coated with a layer of zinc acetate dissolved in 2-methoxyethanol, which would turn into an amorphous ZnO layer (~20 nm) upon gentle annealing to improve electron transport across the interlayer.[24,34] Next, the two subcells are directly glued together and annealed at 150 °C. This annealing step can further increase the electrical conductivity of the interconnect and improve the adhesion between the two subcells. Finally, the PDMS stamp is peeled off from the rear cell for depositing the top metal electrodes. It is crucial to have a sticky interconnect to avoid incomplete transfer or fragmentation of the rear cell during peeling.

In the cross-sectional scanning electron microscopy (SEM) image of the resulting tandem cell (Figure 5a), an interface between the two subcells can be clearly seen without observable interlayer mixing. Electrons from the front cell can be recombined with the holes from the rear cell at the interface made of a layer of amorphous ZnO and the annealed GO/PEDOT, leading to the combined V_{oc}. As shown in Figure 5b, the V_{oc}s of separately prepared front and back subcells are 0.59 and 0.53 V, respectively. The V_{oc} of the tandem cell is 0.94 V, reaching 84% of the sum of the subcell V_{oc}. This proves that the two subcells have been successfully connected in series, as shown in Figure 5b. The power conversion efficiency (PCE) of the final tandem cell is calculated to be 4.14%, which is higher than that of either of the two cells (2.92% and 3.75%, respectively). The J_{sc} of the tandem device using the same polymer is limited by the current of the less absorbing rear cell. This prevents our model system from achieving even higher efficiency. However, we shall point out that this is not a problem associated with the interlayer. Control devices using PEDOT:PSS as the interconnect without GO were also fabricated by direct adhesive lamination. However, all these devices showed lower V_{oc} and PCE than single-layer devices. We attribute this to the inefficient separation of the two cells, which essentially turned the tandem device into a thickened single-layer device with much higher internal resistance. GO is essentially a 2D cross-linked polymer, and its barrier property makes it perfectly suited for preventing intermixing in solution-processed tandem cells.

With the development of new absorbers and adducts,[35] the efficiency of organic solar cells has been rapidly improved.

dx.doi.org/10.1021/ja203464n | J. Am. Chem. Soc. 2011, 133, 9262–9265

Multijunction cells offer a parallel approach to improve efficiency from the aspect of device architecture. The water-based sticky interconnect and the associated adhesive lamination process could transform the serial layer-by-layer fabrication of tandem devices into a parallel mode, in which the subcells can be independently fabricated and adjusted to balance their photocurrents for achieving high efficiency. This serial-to-parallel transition can reduce the number of sequential fabrication steps, thus significantly improving the yield of devices. The sticky interconnect should integrate well with solar cells using other polymers, small organic molecules, or even inorganic nanoparticles, leading to a diverse array of tandem solar cells with different material combinations.

In conclusion, mixing GO and conducting polymer PEDOT:PSS aqueous dispersions results in greatly increased solution viscosity, which can yield an adhesive composite with significantly higher electrical conductivity. The insulating GO makes the PEDOT polymer more conductive by altering its resonating ground states and morphology through strong $\pi-\pi$ interaction and hydrogen bonding. The 2D random diblock copolymer nature of GO could be further explored to guide the assembly of many other materials. The sticky GO/PEDOT interconnect layer greatly facilitates the construction of solution-processed tandem solar cells through direct adhesive lamination, which helps to eliminate the constraint imposed by orthogonal solubility during solution processing. It could also function as nonmetallic solder to electrically, mechanically, and optically connect parts in other organic electronic devices.

■ ASSOCIATED CONTENT

Supporting Information. Experimental details and supplementary data. This material is available free of charge via the Internet at http://pubs.acs.org.

■ AUTHOR INFORMATION

Corresponding Author
jiaxing-huang@northwestern.edu

■ ACKNOWLEDGMENT

The authors thank ISEN (booster award), NSF (DMR CAREER 0955612), the Sony Corporation, and the Northrop Grumman Corporation for supporting this research, Prof. S. I. Stupp for use of his photovoltaic device fabrication and measurement system, M. Seniw at CLAMMP for assistance with mechanical measurements, NUANCE for use of their microscopy facilities, and T. H. Kuo, C-W. Chu, J. Luo, K. Sohn, and T. H. Han for helpful discussions.

■ REFERENCES

(1) Brodie, B. C. *Philos. Trans. R. Soc. London* **1859**, *149*, 249–259.
(2) Hummers, W. S.; Offeman, R. E. *J. Am. Chem. Soc.* **1958**, *80*, 1339–1339.
(3) Novoselov, K. S.; Geim, A. K.; Morozov, S. V.; Jiang, D.; Zhang, Y.; Dubonos, S. V.; Grigorieva, I. V.; Firsov, A. A. *Science* **2004**, *306*, 666–669.
(4) Schniepp, H. C.; Li, J. L.; McAllister, M. J.; Sai, H.; Herrera-Alonso, M.; Adamson, D. H.; Prud'homme, R. K.; Car, R.; Saville, D. A.; Aksay, I. A. *J. Phys. Chem. B* **2006**, *110*, 8535–8539.
(5) Li, D.; Kaner, R. B. *Science* **2008**, *320*, 1170–1171.
(6) Park, S.; Ruoff, R. S. *Nature Nanotechnol.* **2009**, *4*, 217–224.
(7) Compton, O. C.; Nguyen, S. T. *Small* **2010**, *6*, 711–723.
(8) Loh, K. P.; Bao, Q. L.; Eda, G.; Chhowalla, M. *Nature Chem.* **2010**, *2*, 1015–1024.
(9) Stankovich, S.; Dikin, D. A.; Piner, R. D.; Kohlhaas, K. A.; Kleinhammes, A.; Jia, Y.; Wu, Y.; Nguyen, S. T.; Ruoff, R. S. *Carbon* **2007**, *45*, 1558–1565.
(10) Luo, J.; Cote, L. J.; Tung, V. C.; Tan, A. T. L.; Goins, P. E.; Wu, J.; Huang, J. *J. Am. Chem. Soc.* **2010**, *132*, 17667–17669.
(11) Su, C. Y.; Xu, Y. P.; Zhang, W. J.; Zhao, J. W.; Tang, X. H.; Tsai, C. H.; Li, L. J. *Chem. Mater.* **2009**, *21*, 5674–5680.
(12) Cote, L. J.; Kim, F.; Huang, J. X. *J. Am. Chem. Soc.* **2009**, *131*, 1043–1049.
(13) Kim, J.; Cote, L. J.; Kim, F.; Yuan, W.; Shull, K. R.; Huang, J. X. *J. Am. Chem. Soc.* **2010**, *132*, 8180–8186.
(14) Cote, L. J.; Kim, J.; Tung, V. C.; Luo, J. Y.; Kim, F.; Huang, J. X. *Pure Appl. Chem.* **2011**, *83*, 95–110.
(15) Kim, F.; Cote, L. J.; Huang, J. X. *Adv. Mater.* **2010**, *22*, 1954–1958.
(16) Kim, J. E.; Han, T. H.; Lee, S. H.; Kim, J. Y.; Ahn, C. W.; Yun, J. M.; Kim, S. O. *Angew. Chem., Int. Ed.* **2011**, *50*, 3043–3047.
(17) Lerf, A.; He, H. Y.; Forster, M.; Klinowski, J. *J. Phys. Chem. B* **1998**, *102*, 4477–4482.
(18) Gao, W.; Alemany, L. B.; Ci, L. J.; Ajayan, P. M. *Nature Chem.* **2009**, *1*, 403–408.
(19) Erickson, K.; Erni, R.; Lee, Z.; Alem, N.; Gannett, W.; Zettl, A. *Adv. Mater.* **2010**, *22*, 4467–4472.
(20) Kirchmeyer, S.; Reuter, K. *J. Mater. Chem.* **2005**, *15*, 2077–2088.
(21) Brabec, C. J.; Gowrisanker, S.; Halls, J. J. M.; Laird, D.; Jia, S. J.; Williams, S. P. *Adv. Mater.* **2010**, *22*, 3839–3856.
(22) Ameri, T.; Dennler, G.; Lungenschmied, C.; Brabec, C. J. *Energy Environ. Sci.* **2009**, *2*, 347–363.
(23) Kim, J. Y.; Lee, K.; Coates, N. E.; Moses, D.; Nguyen, T. Q.; Dante, M.; Heeger, A. J. *Science* **2007**, *317*, 222–225.
(24) Chou, C.; Kwan, W. K.; Hong, Z.; Chen, L. M.; Yang, Y. *Adv. Mater.* **2010**, *23*, 1282–1286.
(25) Sista, S.; Park, M. H.; Hong, Z. R.; Wu, Y.; Hou, J. H.; Kwan, W. L.; Li, G.; Yang, Y. *Adv. Mater.* **2010**, *22*, 380–383.
(26) Hadipour, A.; de Boer, B.; Wildeman, J.; Kooistra, F. B.; Hummelen, J. C.; Turbiez, M. G. R.; Wienk, M. M.; Janssen, R. A. J.; Blom, P. W. M. *Adv. Funct. Mater.* **2006**, *16*, 1897–1903.
(27) Kim, F.; Luo, J.; Cruz-Silva, R.; Cote, L. C.; Sohn, K.; Huang, J. *Adv. Funct. Mater.* **2010**, *20*, 2867–2873.
(28) Choi, K. S.; Liu, F.; Choi, J. S.; Seo, T. S. *Langmuir* **2010**, *26*, 12902–12908.
(29) Bon, S. B.; Valentini, L.; Kenny, J. M. *Chem. Phys. Lett.* **2010**, *494*, 264–268.
(30) Jo, K.; Lee, T.; Choi, H. J.; Park, J. H.; Lee, D. J.; Lee, D. W.; Kim, B. S. *Langmuir* **2011**, *27*, 2014–2018.
(31) Chang, H. X.; Wang, G. F.; Yang, A.; Tao, X. M.; Liu, X. Q.; Shen, Y. D.; Zheng, Z. J. *Adv. Funct. Mater.* **2010**, *20*, 2893–2902.
(32) Ouyang, J.; Xu, Q. F.; Chu, C. W.; Yang, Y.; Li, G.; Shinar, J. *Polymer* **2004**, *45*, 8443–8450.
(33) Tung, V. C.; Huang, J.-H.; Tevis, I.; Kim, F.; Kim, J.; Chu, C.-W.; Stupp, S. I.; Huang, J. *J. Am. Chem. Soc.* **2011**, *133*, 4940–4947.
(34) Sekine, N.; Chou, C. H.; Kwan, W. L.; Yang, Y. *Org. Electron.* **2009**, *10*, 1473–1477.
(35) Lee, J. M.; Park, J. S.; Lee, S. H.; Kim, H.; Yoo, S.; Kim, S. O. *Adv. Mater.* **2011**, *23*, 629–633.